Optica Applicata, Vol. XLIII, No. 4, 2013
DOI: 10.5277/oa130416

Tunable diode laser spectrometry signal de-noising using discrete wavelet transform for molecular spectroscopy study

GUANG TIAN[1], JINGSONG LI[2*]

[1]School of Science, Tianjin University of Technology and Education, 300222 Tianjin, China

[2]Key Laboratory of Opto-Electronic Information Acquisition and Manipulation of Ministry of Education, Anhui University, Hefei, 230601, China

[*]Corresponding author: ljs0625@126.com

Wavelet-based digital signal processing technique was applied successfully to tunable diode laser absorption spectroscopy (TDLAS) in the infrared spectral range. By applying the wavelet-based digital signal processing technique to simulated and real TDLAS signals, spectral signal-to-noise ratios have been significantly enhanced, which is very useful for atmospheric trace gas detection and molecular spectroscopy study. It is worth specially pointing out that the determined precision of spectroscopic parameters by wavelet-based de-noising technique was distinctly improved, especially for the spectra corrupted by the annoying etalon fringes. Typically, the fitting precision of 2–5 times was achieved for the selected absorption line P10e of CO_2 near 2.064 μm. The primary results show that the proposed filtering technique have a great potential for various laser spectroscopy applications.

Keywords: tunable diode laser absorption spectroscopy (TDLAS), wavelet transform, molecular spectroscopy.

1. Introduction

Removing or deducing noise levels is a very important task in laser spectroscopy for obtaining highly accurate data. A differential absorption technique is the most common method used for suppressing noises in laser absorption spectrometry [1], it involves splitting the light signal into an absorption signal and a reference signal. In theory, this technique assumes that the noises have equal effects on both signal channels by subtracting or dividing the two signals to remove excess noises. In practice, such assumption is not always correct and therefore using a receiver or divider does not provide the expected results. Moreover, the most common method for increasing the signal-to-noise ratios (SNR) in laser absorption spectrometry is to chop the laser beam or modulate the laser current and detect the signal with a look-in amplifier (also known as a phase-sensitive detector). This technique (including amplitude modulation,

wavelength modulation and (or two-tone) frequency modulation) [2–4] provides very good results but its implementation requires a very sophisticated electro-optical design. Another approach is a multi-signal averaging technique [4]. Generally, for the typical white noise, it can be reduced up to the limits of the instrument stability, thus to gain a satisfactory SNR by averaging a set of laser scans. The optimal stability time before the instrument drifts, the influence of the averaging can be determined by the Allan variance technique [5]. However, the multi-signal averaging technique is time consuming and thus unsuitable for some special applications which require a high temporal resolution.

An alternative for improving instrumental precision and accuracy is to digitally process signals delivered by the measuring equipment. From a practical standpoint, numeric filtering is easy to implement, since it requires no modifications or additions to the apparatus hardware and can be easily adapted to any experimental configuration. Mathematical filtering techniques for on-line noise reduction or off-line data processing of recorded spectra may be a better choice when temporal resolution is crucial.

Traditional filtering techniques in most cases rely on the identification of frequencies of noise contributions obtained in the stationary power spectrum. For example, Gaussian filter and Wiener filter exploit prior knowledge of parameters characterizing the noise, specifically the mean and variance. In recent years, wavelet transform has become very popular in many application fields such as physics, engineering, biomedical, signal processing, mathematics and statistics. Wavelet transform has been proved as a powerful tool for signal processing mainly due to its multi-resolution characteristics, *i.e.*, dividing the frequency contents of a signal into low and high sub-bands. Unlike the Fourier transform which considers only a single set of basis functions (sines or cosines), wavelet transforms use an infinite set of possible basis functions (*i.e.*, mother wavelets) with different properties. Thus, wavelet analysis provides immediate access to information that can be obscured to other time-frequency methods such as Fourier analysis. According to the pertinent literature [6], there is a tendency to use wavelet filters to filtrate spectroscopic signals as they provide multi-resolution analysis in both time and frequency domains, and preserve the characteristics of the original signal to the greatest extent [7–10].

In this paper, we present a new approach (*i.e.*, wavelet based filtering) for eliminating or minimizing various noise sources (such as Gaussian, optical fringe noise, *etc*.) commonly encountered in a tunable diode laser absorption spectrometer (TDLAS) which can be used for quantifying trace gas concentration measurement or molecular spectroscopy study. The ultimate goal was to improve the TDLAS spectral SNR, further to increase system sensitivity, measurement precision and accuracy; wavelet transform-based digital filtering was thus used. To facilitate evaluating this technique, it was applied to artificially created CO_2 absorption signals and real TDLAS signals. Spectral SNR was quantified and compared with different thresholding policy and against a traditional filter approach.

2. Wavelet-based filtering

The continuous wavelet transform (CWT) is computed by changing the scale of the analysis window, shifting the window in time, multiplying by the signal, and integrating over all times. The CWT of a signal $x(t)$ is given by [11]:

$$W_f(\tau, s) = \frac{1}{\sqrt{|s|}} \int_{-\infty}^{+\infty} x(t) \Psi\left(\frac{t-\tau}{s}\right) \mathrm{d}t \tag{1}$$

where τ and s are the so-called translation (or time location) factor and the scaling (or dilation) factor, respectively. The factor $|s|^{-1/2}$ is for energy normalization across the different scales, whereas $\Psi_{\tau, s}(t)$ is the so-called *continuous wavelet* or *mother wavelet*:

$$\Psi_{\tau, s}(t) = \frac{1}{\sqrt{|s|}} \Psi\left(\frac{t-\tau}{s}\right)$$

For each scale s and location τ, the wavelet coefficient $W_f(\tau, s)$ represents the information contained in $f(t)$ at that scale and position.

Discrete wavelet transform (DWT) coefficients are usually sampled from the CWT on a dyadic grid, by choosing parameters of translation $\tau = n2^m$, and scale $s = 2^m$, thus the mother wavelet in DWT (*i.e.*, discrete wavelet) is defined by:

$$\Psi_{m, n}(t) = \frac{1}{\sqrt{2^m}} \Psi\left(\frac{t - n2^m}{2^m}\right) \tag{2}$$

DWT analyzes the signal by decomposing it into its approximation and detailed information, which is accomplished by using successive high-pass and low-pass filtering operations, on the basis of the following equations:

$$y_{\text{high}}(k) = \sum_n x(n) g(2k-n) \tag{3}$$

$$y_{\text{low}}(k) = \sum_n x(n) h(2k-n) \tag{4}$$

where $y_{\text{high}}(k)$ and $y_{\text{low}}(k)$ are the outputs of the high-pass and low-pass filters with impulse response g and h, respectively, after subsampling by 2. This procedure is repeated for further decomposition of the low-pass filtered signals. A so-called pyramid algorithm introduced by Mallat for calculating DW coefficients is widely used for signal processing [12]. Starting from the approximation and detailed coefficients, the inverse discrete wavelet reconstructs the signal, inverting the decomposition step by inserting zeros and convolving the results with the reconstruction filters. Therefore, the whole WT process involves signal analysis and reconstruction, *i.e.*, wavelet analy-

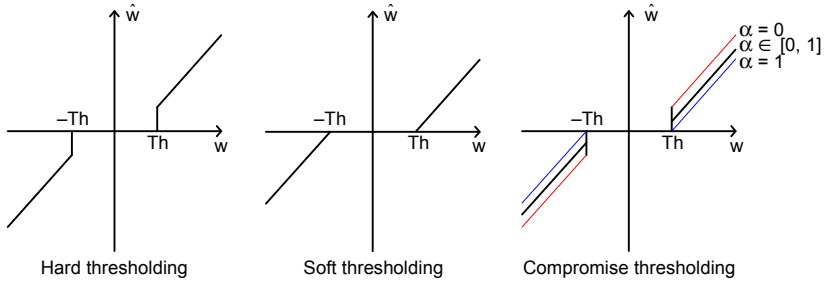

Fig. 1. Thresholding policy of wavelet coefficients.

sis involves filtering and down sampling while reconstruction involves oversampling (up sampling) and filtering. Finally, we can recover the signal by applying the inverse discrete wavelet transform (IDWT) to the thresholded coefficients.

Usually, two different thresholding approaches are applied to signal de-noising: hard thresholding or soft thresholding [13]. The hard thresholding method consists in setting all the wavelet coefficients below a given threshold to zero, while in soft thresholding the wavelet coefficients are reduced by a quantity equal to the threshold value. The so-called soft thresholding function has the well-known and desirable properties of smoothness and adaptation, which might reduce the signal amplitude due to the constant presence of a bias at the wavelet coefficients w higher than the threshold ($|w| > \mathrm{Th}$). The hard thresholding operation keeps the amplitude constant before and after de-noising, but might induce some Gibbs oscillation at the edges due to its discontinuity. In view of these issues, a compromise thresholding policy has been proposed on the signal processing in this paper, as shown in Fig. 1. Their mathematical expressions are given as:

– Hard thresholding:

$$f_{\mathrm{hard}}(t) = \begin{cases} f(t) & \text{for} \quad |f(t)| > \mathrm{Th} \\ 0 & \text{for} \quad |f(t)| \le \mathrm{Th} \end{cases} \tag{5}$$

– Soft thresholding:

$$f_{\mathrm{soft}}(t) = \begin{cases} \mathrm{sign}\Big(f(t)\Big)\Big[|f(t)| - \mathrm{Th}\Big] & \text{for} \quad |f(t)| > \mathrm{Th} \\ 0 & \text{for} \quad |f(t)| \le \mathrm{Th} \end{cases} \tag{6}$$

– Compromise thresholding:

$$f_{\mathrm{compromise}}(t) = \begin{cases} \mathrm{sign}\Big(f(t)\Big)\Big[|f(t)| - \alpha \times \mathrm{Th}\Big] & \text{for} \quad |f(t)| > \mathrm{Th} \\ 0 & \text{for} \quad |f(t)| \le \mathrm{Th} \end{cases} \tag{7}$$

Among them $\alpha \in [0, 1]$, which is the on-soft and hard compromise threshold of a wavelet coefficients estimator. When $\alpha = 0$ or $\alpha = 1$ it becomes a hard and soft threshold method, respectively. For general terms $\alpha \in [0, 1]$, the method estimated the threshold coefficient between hard and soft methods.

There are many possible approaches to estimate the threshold [14]. The universal threshold known as the most popular one is based on statistical properties of white Gaussian noise, and is used in our study, which is defined as $\mathrm{Th} = \sigma[2\log(N)]^{1/2}$, where N is the signal length and σ is the standard deviation of the noise, which can be estimated from the median of the detailed coefficients at the first level of signal decomposition $\sigma = |\mathrm{median}(\mathrm{detail})|/0.6745$.

The computations were performed with MATLAB scripting language for Windows version, using our own programs. The MATLAB Toolbox for wavelets was used as the library of wavelet filter coefficients.

3. Results and discussion

3.1. Using wavelet for de-noising of simulated TDLAS signal

A computer program has also been written in the numerical script language MATLAB to simulate the TDLAS absorption profiles under a variety of conditions (including temperature, pressure, gas concentration and optical path length) by extracting related spectroscopic parameters from the Hitran08 database [15]. From the viewpoint of practical applications, a CO_2 absorption line near the wavelength of 4845.64 cm^{-1} was very attractive for atmospheric CO_2 measurements. Therefore, relative spectroscopic simulation of absorption signals covering this spectral region was made. All the simulated signals contain 1024 sample points. To evaluate the performance of the wavelet-based signal filtering technique, each spectrum was purposefully corrupted with Gaussian distributed white noise to simulate an instrument-based signal. Spectra SNR are used as the evaluation criteria and defined as follows:

$$\mathrm{SNR} = 10\log\left[\frac{\mathrm{std}(\mathrm{signal}_{\mathrm{noise\_free}})}{\mathrm{std}(\mathrm{signal}_{\mathrm{noise\_free}} - \mathrm{signal}_{\mathrm{wavelet\_denoised}})}\right] \tag{8}$$

where std means the standard deviation, $\mathrm{signal}_{\mathrm{noise\_free}}$ and $\mathrm{signal}_{\mathrm{wavelet\_denoised}}$ are ideally simulated spectral signal and wavelet filtered spectral signal, respectively.

Figure 2 depicts the basic principle of discrete wavelet decomposition of a simulated TDLAS signal. For decomposition of the signal it is very important to choose a suitable mother wavelet. The shape of the mother wavelet has to be very similar to the signal to be analyzed. Generally, it should fulfill the following properties: symmetry, orthogonality and feasibility for DWT, *etc*. In order to achieve the best performance, a group of mother wavelets has been tested: Daubechie (db) family wavelets (db1 to db20, 20 elements), symlet (sym) family wavelets (sym2 to sym20, 19 elements),

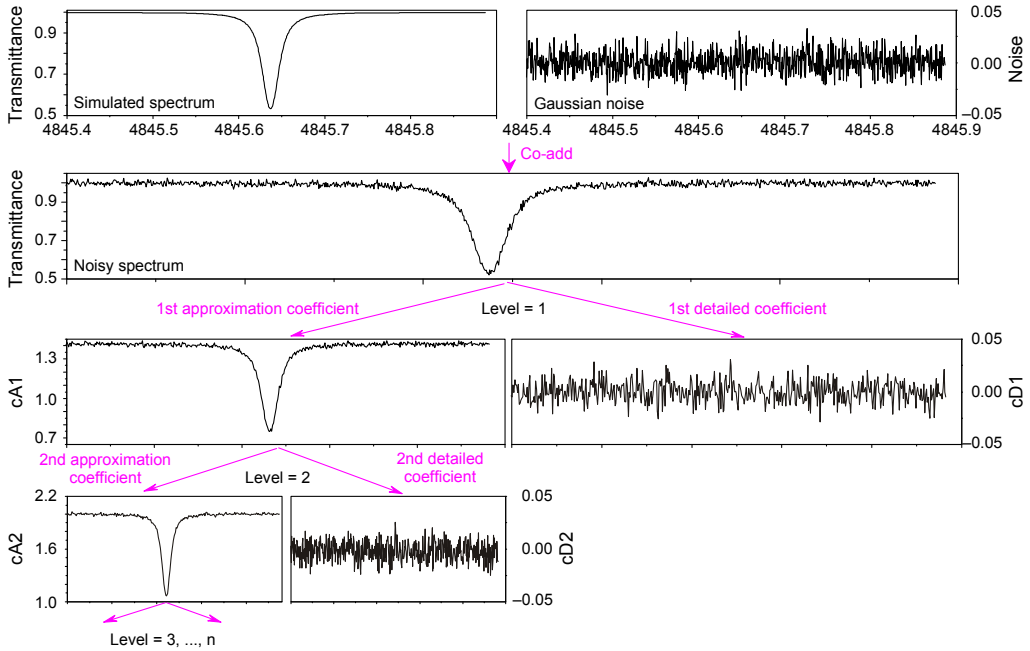

Fig. 2. Principle of discrete wavelet decomposition of a simulated TDLAS signal.

coiflet (coif) family wavelets (coif1 to coif5, 5 elements), biorthogonal (bior) and reverse biorthogonal (rbio) family wavelets (bior1.1 to bior6.8, 5 elements, and rbio1.1 to rbio6.8, 5 elements), as well as Haar's wavelet (1 element), and the discrete Meyer wavelet (*i.e.*, dmey wavelet, 1 element).

As an example, Fig. 3 shows the simulated signal under different noise levels and wavelet db10 filtered results with compromise thresholding (for this study $\alpha = 0.5$). For comparison, the filtered results of the classic filter technique, *i.e.*, fast Fourier transform (FFT), were also presented. It is obvious that the wavelet filter shows the best results and keeps the maximum approximation degree. The calculated SNR corresponding to each case is also inset in the corresponding panel. After many experimental trials with each wavelet family, the best wavelets and their performance under different thresholding policy are complied in Tab. 1. As can be seen from this table, the proposed compromise thresholding is superior to other two commonly used methods. Obviously, the enhancement factor of SNR depends on the noise level, the poorer the original signal, the higher the SNR gain factor. Moreover, we found that the optimal decomposition levels have slightly shifted between level 5 and 7 following the variation of the SNR. It is worth mentioning that the purpose of an optimal filter is to recover the de-noised signal without degrading the approximation degree between the real signal and the reconstructed signal. Wavelet-based filtering is a data dependent process. Improper choice of the mother wavelet can cause distortions and artefacts in the reconstructed signal, such as haar wavelet (not shown here) [16, 17]. In addition, sometimes the difference of the best SNR obtained between the so-called optimal

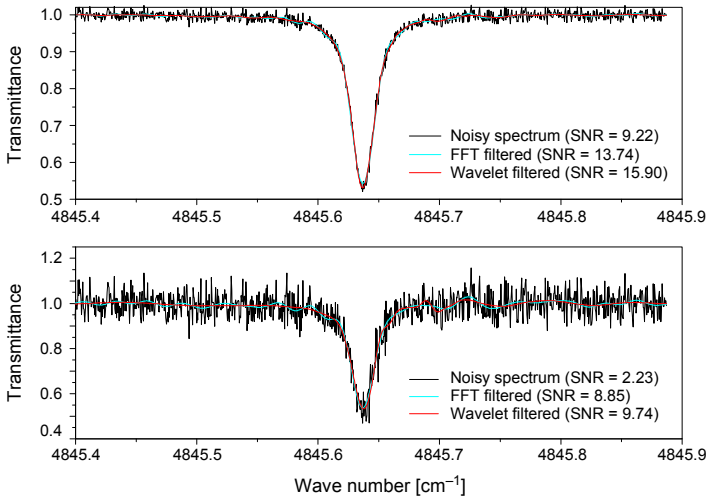

Fig. 3. Comparison of simulated noisy transmittance signals and db10 wavelet filtered results with compromise thresholding ($\alpha = 0.5$).

wavelet and others is really very small, as can be seen from Tab. 1. Nevertheless all the mother wavelets listed in the Tab. 1 except dmey and haar wavelet can be selected as a good candidate for de-noising applications to the experimental TDLAS spectra in this work.

T a b l e 1. The best SNR obtained by the optimal wavelet in each wavelet family under different thresholding policy and the corresponding optimal decomposition level.

Wavelet	Raw_SNR	Thresholding			Gain factor	Optimal decomposition level
		Soft	Hard	Compromise		
db10	9.22	15.24	15.31	15.90	1.72	5
sym17		15.02	15.09	15.72	1.70	5
coif2		15.12	15.18	15.94	1.73	6
bior2.8		15.24	15.36	15.54	1.68	7
rbio5.5		15.24	15.32	15.58	1.69	7
dmey		14.35	14.39	14.55	1.58	5
haar		12.45	12.39	12.65	1.37	6
db10	2.23	9.17	9.34	9.74	4.36	6
sym17		8.97	9.09	9.35	4.17	6
coif2		9.33	9.52	9.88	4.42	6
bior2.8		8.97	9.20	9.23	4.13	7
rbio5.5		9.18	9.44	9.59	4.29	7
dmey		8.70	8.77	8.16	3.65	6
haar		7.47	7.50	7.67	3.43	6

Note: Gain factor = Compromise thresholding/Raw_SNR.

3.2. Using wavelet for de-noising of real TDLAS signal

For further evaluation of the wavelet-based filtering technique for noise reduction, we applied the proposed wavelet algorithm (db10 wavelet with compromise thresholding $\alpha = 0.5$) to actually recorded CO_2 absorption spectra. The experimental set-up is similar to Lepère's system [18]. The measured TDLAS signals are very noisy, especially corrupted by the optical etalon fringes. Figure 4 presents a typical application of wavelet filtering to an experimentally recorded CO_2 absorption spectrum near 4845.64 cm^{-1} and corresponding Voigt fit (lower panel). For clarity, a zoom-in data between 4845.2–4845.4 cm^{-1} (upper panel) illustrates the detailed comparison. As can be seen, after the application of wavelet filtering, the annoying etalon fringes which often occurred in TDLAS system have been significantly removed. The calculated SNR before and after wavelet filter are 13.07 and 17.08, respectively. Thus a SNR enhancement factor of 1.31 is obtained. These results prove that the proposed wavelet filter in this work is a very effective de-nosing tool not only for common Gaussian noise but also for optical etalon fringes.

The present work aims to demonstrate wavelet-based filtering for TDLAS spectral signal improvement for molecular spectroscopy study (*i.e.*, spectroscopic parameters measurement), and currently no attempt has been made to optimize the sensitivity of

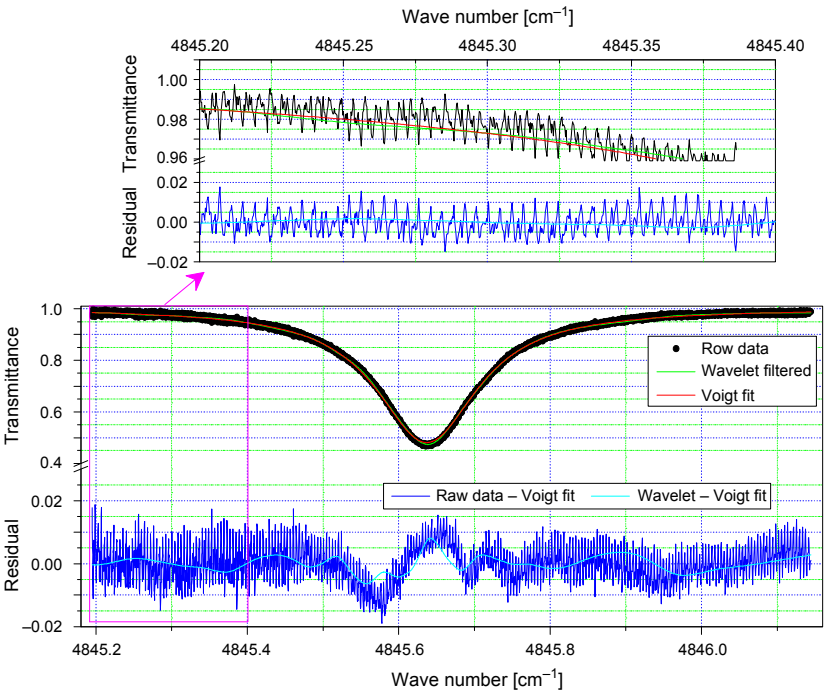

Fig. 4. Typical example of experimentally determined TDLAS signal (pressure = 836.47 mbar, path length = 2400 cm, mixing ratio = 1.49%) and db10 wavelet filtered results with compromise thresholding ($\alpha = 0.5$). For clarity, a zoom-in data between 4845.2–4845.4 cm^{-1} (upper panel) illustrates the detailed comparison.

the TDLAS system for trace gas detection. To perform precise line shape studies, it is necessary to have enough spectral SNR, thus spectroscopic parameters can be retrieved with high precision and accuracy. For this purpose, series of experimental spectra of line transition P10e of CO_2 between 4845 and 4846.5 cm^{-1} under different conditions are recorded, and the standard Voigt model is used to fit the experimental CO_2 absorption spectra before and after the application of a wavelet filter for line intensity and air-broadening coefficients determination.

To determine the absolute line intensity, the CO_2 absorbance was numerically integrated over the entire spectral contour, the fitted integrated absorbance area A was divided by the product of the CO_2 concentration and the path length to obtain the line intensity at experimental temperature, then converted to the standard temperature using the lower state energy and the vibrational and rotational partition functions for intercomparison. However, an air-broadening coefficient can be directly determined form the slope of the fitted Lorentzian line width *versus* pressure. A detailed description of the fitting procedure used for the analysis of the spectra and the data reduction can be found in related publications [19].

Figure 5 shows a typical application of a wavelet filter on a mixture spectrum of CO_2 in air at the pressure of 762.20 mbar and mixing ratio of 1.54%. The upper panel

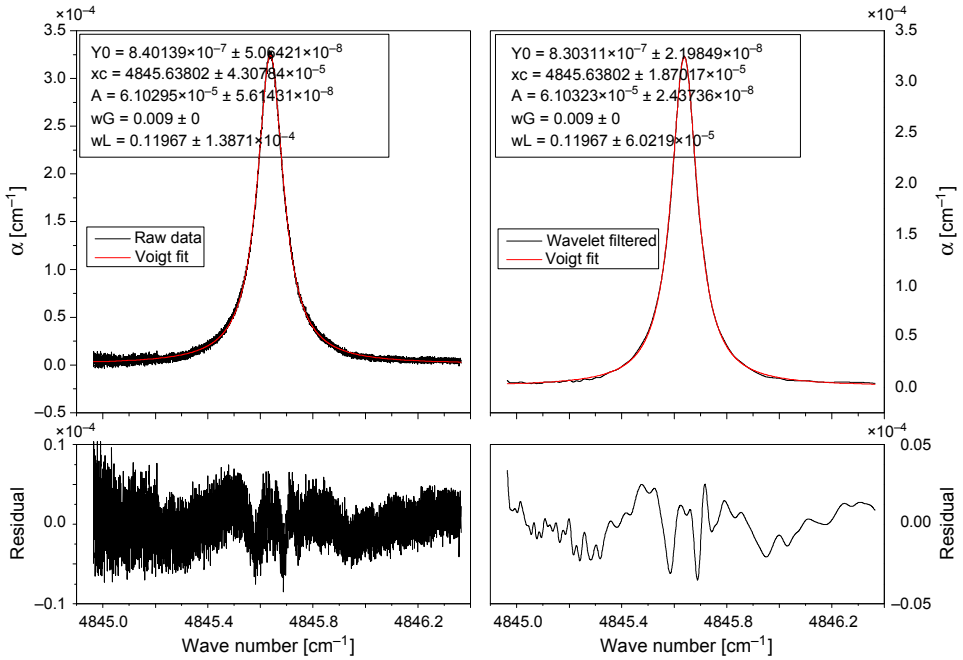

Fig. 5. An example of the application of wavelet filter on a CO_2 absorption spectrum under the experimental conditions of pressure = 762.20 mbar, CO_2 mixing ratio in air = 1.54%, temperature = = 293 K. The smooth curve is the best-fitted curve with the Voigt profile function. Lower panel shows the corresponding residuals. The fitted parameters are also inset in the corresponding panel, Y_0 denotes background offset, x_c means absorption line central position, A means the integrated absorbance area, w_G and w_L are Doppler and Lorentzian FWHM (full width at half maximum), respectively.

shows the raw experimental spectrum (upper left panel) and wavelet filtered spectrum (upper right panel), the smooth curve is the best-fitted curve with the Voigt profile function. The lower panel shows the residuals of the raw experimental spectrum (bottom left panel) and wavelet filtered spectrum (bottom right panel), respectively. The fitted parameters are also inset in the corresponding panel. From this figure, we can see that the spectral SNR has been significantly improved after the application of the wavelet filter. The fitted spectroscopic parameters are almost identical, but the fit precisions of those with the application of the wavelet filter are obviously better than those without the application of the wavelet filter. The same procedure is also followed for the other experimental spectra recorded under different pressures.

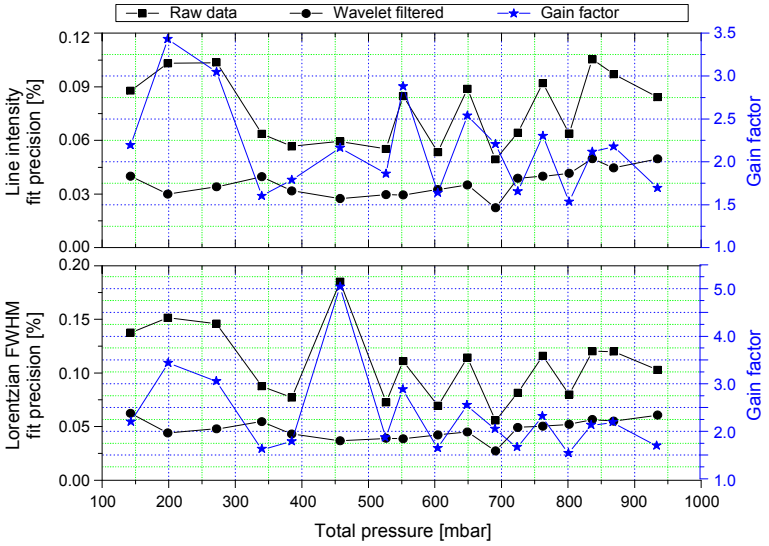

Fig. 6. The fitting precisions of line intensity (upper panel, left axis) and Lorentzian FWHM (lower panel, right axis) in both cases (with and without wavelet filter) for the line transition P10e of CO_2 as a function of total pressure, as well as the corresponding enhancement factor (unfiltered/filtered, right axis).

For better comparison, Fig. 6 presents the fit precisions in both cases (with and without the wavelet filter) and the corresponding enhancement factors (unfiltered/filtered) of fit precisions as a function of total sample pressures. From this figure, we can see that the fit precision enhancement between 1.5 and 3.5 for line intensity, and from 1.5 to 5.5 for Lorentzian FWHM (full width at half maximum) depends on noisy spectral characteristics have been achieved. Note that the W-shaped residuals that occurred at the absorption line center (see Fig. 5) can be effectively removed by using advanced line shape models, such as Rautian profile [20] and Galatry profile [21], which take into account the Dicke narrowing effect, lead to a better fit than the one obtained from the Voigt profile [22].

Finally, the absolute line intensity and the air-broadening coefficient of CO_2 line transition P10e near 4845.64 cm^{-1} achieved before and after the application of

T a b l e 2. Line intensity and air-broadening coefficient of CO_2 P10e line transition obtained with and without wavelet filter, and comparison with the main atmospheric database Hitran08.

Line intensity at 296 K [$\times 10^{-22}$ cm^{-1}/(molecule×cm^{-2})]			Line position [cm^{-1}]
	Hitran08	2.125	4845.637
This work	Raw data	2.101	
	Uncertainties [%]	0.077	
	Discrepancies [%]	–1.129	
	Wavelet	2.104	
	Uncertainties [%]	0.036	
	Discrepancies [%]	–0.899	
Air-broadened coefficients [cm^{-1}/atm]			
	Hitran08	0.0816	4845.637
This work	Raw data	0.0812	
	Uncertainties [%]	0.108	
	Discrepancies [%]	–0.490	
	Wavelet	0.0814	
	Uncertainties [%]	0.047	
	Discrepancies [%]	–0.245	

Note: The reported uncertainty corresponds to one standard deviation obtained by averaging different measurements; Discrepancies is the error percentage ratio defined as [(Hitran08 data – this work)/(Hitran08 data)]×100%.

the wavelet filter in this study are summarized in Tab. 2 and compared with the main atmospheric database Hitran08. For each item, our uncertainty corresponds to one standard deviation obtained by averaging different measurements. The discrepancies between our results and Hitran08 data are also presented in Tab. 2. Both CO_2 spectroscopic parameters (line intensity and air-broadening coefficients) determined before and after the application of the wavelet filter are in quite a good agreement with Hitran08 values. The slight discrepancy is mainly due to TDLAS spectral baseline process, and errors result from some experimental parameters (temperature, path length and pressure) measurements. Anyway, data obtained with the wavelet filter show better uncertainty and discrepancy. Indeed, for those data with poorer SNR, the efficiency of the wavelet filter is more prominent.

4. Summary, conclusions and outlook

Digital signal processing is easy to implement and well adapted to various experimental configurations without any physical modifications or additions to the TDLAS system. The application of wavelet filtering for TDLAS is presented on the example of infrared absorption spectroscopy of CO_2 transition P10e near 2.064 μm. By applying the wavelet-based digital signal processing techniques to simulated and real TDLAS signals, spectral SNR have been significantly enhanced depending upon the qualities of origi-

nal signals and noise characteristics. For molecular spectroscopy study, the retrieval precisions of CO_2 spectroscopic parameters after the application of the wavelet filter were distinctly improved. The results achieved in this study prove that the proposed wavelet-based filter is a very effective de-nosing tool not only for common Gaussian distributed white noise but also for the annoying optical etalon fringes.

We are currently improving this technique and integrating an adaptive matched filter (such as Kalman filter [23]) with the proposed wavelet filter for atmospheric trace gas sensing and other applications. Furthermore, we are taking great care in the baseline correction and normalization of TDLAS spectra by wavelet transform to avoid artificial bias and drifts as well as other interfering sources, since the contribution of the wings of the absorption profile (especially for weak absorption) could be underestimated or overestimated during the baseline processing and normalization [24], which is very important for the estimation of an unbiased integrated absorption area of the absorption line in molecular spectroscopy study. These primary results show that the proposed filtering technique have a great potential for other laser spectroscopy applications, high-precision analysis of atmospheric trace gases, isotope ratio and eddy covariance measurements.

Acknowledgments – This work was supported by Anhui University Personnel Recruiting Project of Academic and Technical Leaders (Grant No. 10117700014). The authors gratefully acknowledge the anonymous reviewers and editors for their valuable comments and suggestions to improve the quality of the paper.

References

[1] JIMÉNEZ R., TASLAKOV M., SIMEONOV V., CALPINI B., JEANNERET F., HOFSTETTER D., BECK M., FAIST J., VAN DEN BERGH H., *Ozone detection by differential absorption spectroscopy at ambient pressure with a 9.6 μm pulsed quantum-cascade laser*, Applied Physics B: Lasers and Optics **78**(2), 2004, pp. 249–256.

[2] MENGLONG CONG, SHUXU GUO, YIDING WANG, *A novel methane detection system based on InGaAsP distributed feedback laser*, Optica Applicata **41**(3), 2011, pp. 639–648.

[3] BOMSE D.S., STANTON A.C., SILVER J.A., *Frequency modulation and wavelength modulation spectroscopies: comparison of experimental methods using a lead-salt diode laser*, Applied Optics **31**(6), 1992, pp. 718–731.

[4] WERLE P., *A review of recent advances in semiconductor laser based gas monitors*, Spectrochimica Acta Part A: Molecular and Biomolecular Spectroscopy **54**(2), 1998, pp. 197–236.

[5] WERLE P., MÜCKE R., SLEMR F., *The limits of signal averaging in atmospheric trace-gas monitoring by tunable diode-laser absorption spectroscopy (TDLAS)*, Applied Physics B: Lasers and Optics **57**(2), 1993, pp. 131–139.

[6] XUE-GUANG SHAO, ALEXANDER KAI-MAN LEUNG, FOO-TIM CHAU, *Wavelet: a new trend in chemistry*, Accounts of Chemical Research **36**(4), 2003, pp. 276–283.

[7] RIRIS H., CARLISLE C.B., WARREN R.E., COOPER D.E., MARTINELLI R.U., MENNA R.J., YORK P.K., GARBUZOV D.Z., LEE H., ABELES J.H., MORRIS N., CONNOLLY J.C., NARAYAN S.Y., *Signal processing strategies in tunable diode laser spectrometers*, Spectrochimica Acta Part A: Molecular and Biomolecular Spectroscopy **52**(8), 1996, pp. 843–849.

[8] BERRY R.J., OZAKI Y., *Comparison of wavelets and smoothing for denoising spectra for two-dimensional correlation spectroscopy*, Applied Spectroscopy **56**(11), 2002, pp. 1462–1469.

[9] GALLOWAY C.M, LE RU E.C., ETCHEGOIN P.G., *An iterative algorithm for background removal in spectroscopy by wavelet transforms*, Applied Spectroscopy **63**(12), 2009, pp. 1370–1376.
[10] DUAN H., GAUTAM A., SHAW B.D., CHENG H.H., *Harmonic wavelet analysis of modulated tunable diode laser absorption spectroscopy signals*, Applied Optics **48**(2), 2009, pp. 401–407.
[11] MALLAT S.G., *A Wavelet Tour of Signal Processing*, 2nd Edition, Academic Press, New York, 1999.
[12] MALLAT S.G., *A theory for multiresolution signal decomposition: the wavelet representation*, IEEE Pattern Analysis and Machine Intelligence **11**(7), 1989, pp. 674–693.
[13] JOHNSTONE I.M., SILVERMAN B.W., *Wavelet threshold estimators for data with correlated noise*, Journal of the Royal Statistical Society: Series B **59**(2), 1997, pp. 319–351.
[14] DONOHO D.L., JOHNSTONE I.M., *Adapting to unknown smoothness via wavelet shrinkage*, Journal of the American Statistical Association **90**(432), 1995, pp. 1200–1224.
[15] ROTHMAN L.S., GORDON I.E., BARBE A., *et al.*, *The HITRAN 2008 molecular spectroscopic database*, Journal of Quantitative Spectroscopy and Radiative Transfer **110**(9–10), 2009, pp. 533–572.
[16] PASTI L., WALCZAK B., MASSART D.L., RESCHIGLIAN P., *Optimization of signal denoising in discrete wavelet transform*, Chemometrics and Intelligent Laboratory Systems **48**(1), 1999, pp. 21–34.
[17] LI J.S., PARCHATKA U., FISCHER H., *Applications of wavelet transform to quantum cascade laser spectrometer for atmospheric trace gas measurements*, Applied Physics B: Lasers and Optics **108**(4), 2012, pp. 951–963.
[18] LEPÈRE M., *Line profile study with tunable diode laser spectrometers*, Spectrochimica Acta Part A: Molecular and Biomolecular Spectroscopy **60**(14), 2004, pp. 3249–3258.
[19] LI J.S., JOLY L., COUSIN J., PARVITTE B., BONNO B., ZENINARI V., DURRY G., *Diode laser spectroscopy of two acetylene isotopologues ($^{12}C_2H_2$, $^{13}C^{12}CH_2$) in the 1.533 μm region for the PHOBOS-Grunt space mission*, Spectrochimica Acta Part A: Molecular and Biomolecular Spectroscopy **74**(5), 2009, pp. 1204–1208.
[20] RAUTIAN S.G., SOBEL'MAN I.I., *Effect of collisions on the Doppler broadening of spectral lines*, Soviet Physics Uspekhi **9**(5), 1967, pp. 701–716.
[21] GALATRY L., *Simultaneous effect of Doppler and foreign gas broadening on spectral lines*, Physical Review **122**(4), 1961, pp. 1218–1223.
[22] LI J.S., DURRY G., COUSIN J., JOLY L., PARVITTE B., ZENINARI V., *Self-broadening coefficients and positions of acetylene around 1.533 μm studied by high-resolution diode laser absorption spectrometry*, Journal of Quantitative Spectroscopy and Radiative Transfer **111**(15), 2010, pp. 2332–2340.
[23] CHIEN-MING CHOU, RU-YIH WANG, *Application of wavelet-based multi-model Kalman filters to real-time flood forecasting*, Hydrological Processes **18**(5), 2004, pp. 987–1008.
[24] SHUO CHEN, DON HONG, YU SHYR, *Wavelet-based procedures for proteomic mass spectrometry data processing*, Computational Statistics and Data Analysis **52**(1), 2007, pp. 211–220.

Received January 7, 2013
in revised form March 28, 2013